Available online at www.sciencedirect.com
ScienceDirect
Journal of Magnetism and Magnetic Materials 320 (2008) e279–e282
www.elsevier.com/locate/jmmm

Characterizing magnetic interactions in Ni nanowires by FORC analysis

T.R.F. Peixoto, D.R. Cornejo*

Instituto de Física, Universidade de São Paulo, 05508-900 São Paulo, SP, Brazil

Available online 21 February 2008

Abstract

Polycrystalline Ni nanowires with different diameters were electrodeposited in nanoporous anodized alumina membranes. First-Order Reversal Curves (FORCs) were measured and FORC distributions were calculated. They clearly showed an asymmetric behavior with a strong maximum at negative interaction fields, evidencing the dominant demagnetizing interactions which depend on the geometry of the nanowires.
© 2008 Elsevier B.V. All rights reserved.

PACS: 75.60.Ej; 75.60.Jk; 75.75.+a

Keywords: Magnetic nanowire; FORC; Demagnetization process; Electrodeposition

1. Introduction

Self-organized arrays of ferromagnetic nanowires show potential feasibility for applications in perpendicular magnetic recording media and high-sensitivity magnetic sensors [1], and are well suited for both experimental and theoretical study of magnetism at nanoscale [1–4]. These systems can be easily synthesized through the method of two-step anodization [5] and subsequent chemical electrodeposition [2,3].

One phenomenological approach that has been topic of renewed interest in magnetic systems is the First-Order Reversal Curves (FORC) analysis [6–11]. FORCs can be experimentally obtained as follows: (a) first, one has to saturate the sample with a field $H_{\max}$; (b) then, set the field H to a return value $H_r < H_{\max}$; (c) then, increase H back to $H_{\max}$, measuring the magnetization; and (d) and repeat steps (b) and (c) for decreasing values of H_r, while $H_r \geqslant -H_{\max}$.

The FORC distribution is, then, defined by $\rho(H_r, H) \equiv -0.5\{\partial^2 M(H_r, H)/\partial H_r \partial H\}$ and performed on the dataset of the measured FORCs. The FORC diagram is a contour plot of ρ on a 45° rotated coordinate system $\{H_c = (H - H_r)/2,\quad H_b = (H + H_r)/2\}$. In these coordinates, ρ can be compared to the statistical distribution of particles from the Preisach model [12], which describes the field-induced reversal of an ensemble of single-domain particles.

Thus, the FORC diagram provides a detailed characterization of the hysteretic response of a system because it evidences dominant magnetic interactions, magnetic after-effects and the annihilation of memory during the demagnetization process.

In this work, a set of samples of Ni nanowires grown in the nanoporous anodized alumina membranes were magnetically characterized by FORC analysis.

2. Experimental details

Thin (0.2 mm) Al foils with 99.997% purity were pretreated in vacuum at 600 °C for 2 h; washed in acetone; electropolished in a $H_2SO_4 + H_3PO_4 + H_2O$ solution; etched in a 3 M NaOH solution and rinsed in deionized water. Later, the foils were anodized in a constant voltage cell containing an aqueous solution of 0.3 M oxalic acid ($H_2C_2O_4$), at 4 °C, using a graphite electrode as cathode. The first anodization was carried out for 1 h and the second for 40 min. Several samples were prepared with anodization voltage V_{an} varying between 15 and 30 V. The electrodepositions were carried out in a solution of 0.1 M $NiSO_4 \cdot 6H_2O + 45\,g/L\,H_3BO_3$, at 55 °C, for 2 min, under 20 V, at 100 Hz.

*Corresponding author. Tel.: +55 11 30916885; fax: +55 11 30916984.
E-mail address: cornejo@if.usp.br (D.R. Cornejo).

0304-8853/$ - see front matter © 2008 Elsevier B.V. All rights reserved.
doi:10.1016/j.jmmm.2008.02.060

The structural characterization was done by Scanning Electron Microscopy (SEM) and X-ray Diffractometry (XRD), with Cu K_{α} radiation. The magnetic characterization was accomplished at 300 K in a 7T-SQUID, with magnetic field applied perpendicularly to the membrane surface.

3. Structural and magnetic characterization

SEM images of the samples were obtained and treated in a suitable image processing software, from where we calculated the mean diameter d_m, the mean interpore distance D_{int} and the density of pores. A linear dependence of d_m and D_{int} with V_{an} was observed, with d_m between 30 and 90 nm and D_{int} between 40 and 110 nm, in agreement with the literature [13,14]. The mean density of pores varies between 10^9 and 10^{10} pores/cm^2. The shape of the pores also varies with V_{an}. Samples made at 30 and 40 V have a more regularly oriented hcp patterns. Below $V_{an} = 30$ V, the pore arrays are predominantly random, whereas above 40 V the pores tend to deform. It is well known that the regularity of the pore array depends on voltage and duration of the first anodization [15–17] and that for high V_{an} the pores tend to diverge from the circular shape [18]. On the other hand, the length of the pores depends solely on the duration of the second anodization [13]. We estimate that our samples have lengths between 5 and 15 μm, yielding an aspect ratio greater than 50.

The XRD patterns confirm the presence of polycrystalline Ni. The (1 1 1) peak of Ni was not detected due to its coincidence with the strong (2 0 0) peak of Al. The grain sizes of Ni were calculated for each crystallographic direction and they were seen to increase with d_m, in the range of 10–22 nm, indicating that the geometry of the pores regulates the grain size of Ni. In this range, the crystallites must be exchanged-coupled single-domain particles, with random orientation of easy axes [2]. Such a magnetic structure can allow non-uniform modes of magnetization reversal [19,20].

The shape uniaxial anisotropy in our samples was confirmed by measuring hysteresis loops in the directions perpendicular and parallel to the wires. An outstanding increase of coercive field H_C and remanence ($M_R > 0.5M_S$), in comparison to bulk Ni, was observed. It is in accordance with Ref. [19]. To obtain the FORC distributions, approximately 20 FORCs with $H_{max} = 3$ kOe were measured for each sample (see Fig. 1a). The FORC distributions were calculated by the method described by Heslop and Muxworthy [11], applying the "extended" FORC definition [7], normalized by the saturation magnetization M_S of each sample and plotted in the $\{H_c, H_b\}$ coordinates. Fig. 2b displays typical results for the sample with $d_m = 38$ nm.

4. Results and discussion

In the classical Preisach model, a distribution of non-interacting single-domain particles is considered, where

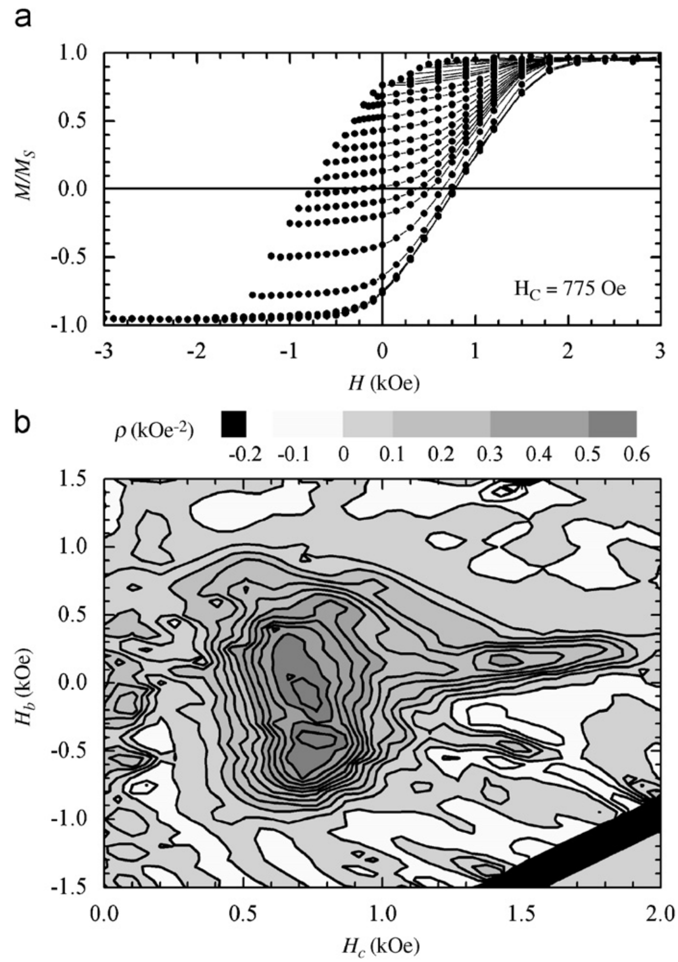

Fig. 1. (a) FORCs and (b) FORC diagram for the sample with $d_m = 38$ nm.

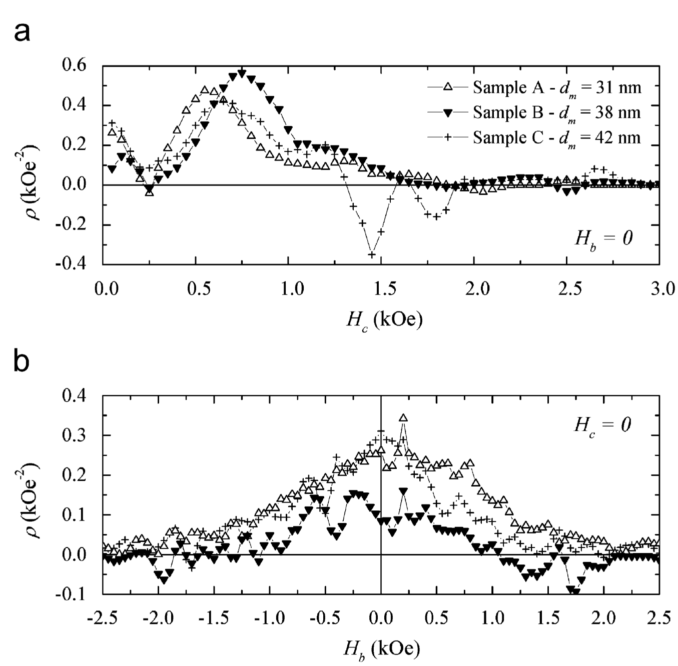

Fig. 2. FORC distribution of all samples at (a) $H_b = 0$ and (b) $H_c = 0$.

each particle is characterized by a square elementary hysteresis loop with width H_c and offset H_b. This distribution $P(H_c, H_b)$ has a definition very similar to that of the FORC distribution [12]. This model only considers magnetization process by irreversible flipping of particles into the direction of the applied field. When particles with zero width are considered, a secondary peak appears at $H_c = 0$ ($H = H_r$) and the main peak is shifted towards the left [6]. Moreover, to have a physical meaning, $P(H_c, H_b)$ has to be positive-valued.

However, real systems exhibit a much more complex magnetic response, resulting from magnetic interactions. In the FORC analysis, the actual behavior of the material is probed and those effects manifest themselves in the FORC diagram, which is a real map of magnetic phenomena in a material.

In our samples, the FORC distributions exhibited the same two-branch structure observed by Pike et al. for a Ni nanopillar array [9] and the splitting of the main peak observed by Muxworthy et al. [8] and Dumas et al. [22]. The most prominent peaks occurred for values of H_c around the coercive field of each sample and for $H_b < 0$. This asymmetry is regarded as the effect of dipolar inter-wire interactions [6]. The nanowire arrays are highly dense, with high aspect ratio (>50). It is expected that they have a strong stray field at the surface, whose lines tend to close into the neighboring wires [2]. Thus, each nanowire experiences a demagnetizing effective interaction field. We can also observe smaller sharp peaks for low values of H_c. As any increase of magnetization in this region is due to the rotation of low-coercivity particles, this magnetization is predominantly reversible, yielding the "reversible ridge" near $H_c = 0$ [7,9]. Negative ρ regions can be also be observed in the diagram. In general, they reflect the fact that in real systems ρ is not uniquely determined by $P(H_c, H_b)$ alone, but also depends on the applied field and the magnetic history of the system [6–9].

Following Ref. [10], we show the behavior of $\rho(H_c, H_b)$ for (a) $H_b = 0$ and (b) $H_c = 0$ for three samples in Fig. 2. In Fig. 2a, each sample exhibits a reversible peak at $H_c = 0$ and an irreversible peak at $H_c > 0$. By comparing the heights and the positions of the peaks, we can notice that reversible processes are stronger in samples A and C than in sample B. In sample C, these two peaks have almost the same height. This sample has the largest mean diameter and the most deformed pores, which can favor non-uniform reversal modes and reversible components. In Fig. 2b, we see the profile of the reversible ridges. The slight asymmetry observed evidences the coupling between reversible and irreversible components [7,9,20]. In Fig. 3a, we plot $\rho(H_b, H_c)$ vs. H_b, at the absolute maximum of each FORC distribution, where the asymmetry towards $H_b < 0$ is stronger.

As several authors have pointed out, the vertical FWHM of the FORC distribution can be regarded as a measure of the mean local interaction field H_{int} among

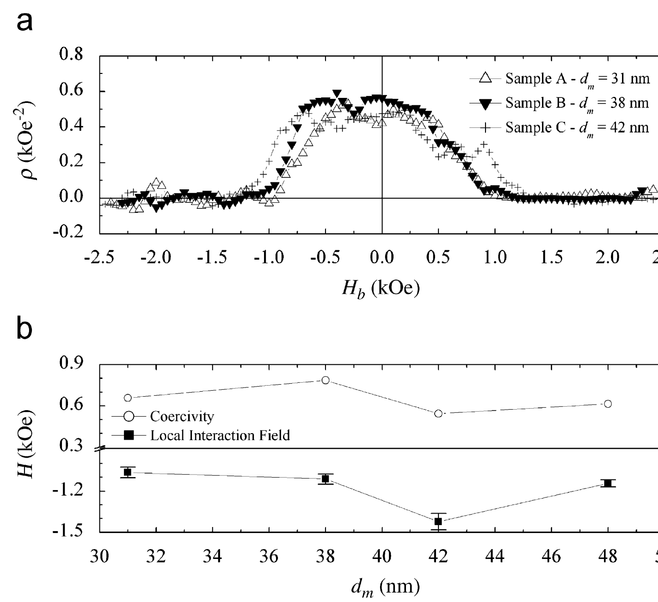

Fig. 3. (a) FORC distributions vs. H_b with H_c fixed at the main irreversible peak and (b) mean local interaction field (H_{int}) and coercivity vs. d_m.

particles [6,8,22]. It represents the spread of the distribution of bias fields H_b. So, the FWHM (H_{int}) was measured for each sample and plotted in Fig. 3b, along with the coercivity of each sample (H_C), as functions of d_m. We can observe that both behaviors seem to be unison with d_m. It is showing that the intensity of the mean local interaction field influences strongly the coercivity of the sample.

5. Conclusions

From the FORC "fingerprints" obtained and based on the extensive literature on the FORC analysis method [2,7,8,10,21,22], we assert that our samples of Ni nanowire arrays do not reverse by coherent rotation alone. A non-uniform reversal mode due to the coupling among Ni grains also occurs, possibly curling [2,19]. Previous M_{rev} vs. M_{irr} curves analysis results for Fe nanowires [20] also corroborate this statement. The intensity of the mean local interaction field, determined from the FORC distribution, influences the coercivity of the sample.

Realistic micromagnetic modeling can also bring complementary knowledge about the magnetization reversal mechanisms of magnetic nanowires. So, a more extensive work regarding these approaches is under way.

Acknowledgments

We are thankful to Dr. Márcia Fantini for her support in the XRD characterization and Dr. David Heslop for private communications. This work was supported by CAPES, CNPq and FAPESP.

References

[1] P.D. McGary, L. Tan, J. Zou, et al., J. Appl. Phys. 99 (2006) 08B310.
[2] D.J. Sellmyer, et al., J. Phys. Condens. Matter 13 (2001) R433.
[3] G. Schmid, J. Mater. Chem. 12 (2002) 1231.
[4] J. Qin, J. Nogués, M. Mikhaylova, et al., Chem. Mater. 17 (2005) 1829.
[5] H. Masuda, K. Fukuda, Science 268 (1995) 1466.
[6] C.R. Pike, A.P. Roberts, K.L. Verosub, J. Appl. Phys. 85 (1999) 6660.
[7] C.R. Pike, Phys. Rev. B 68 (2003) 104424.
[8] A.R. Muxworthy, D. Heslop, W. Williams, Geophys. J. Int. 158 (2004) 888.
[9] C.R. Pike, et al., Phys. Rev. B 71 (2005) 134407.
[10] J.E. Davies, J. Wu, C. Leighton, et al., Phys. Rev. B 72 (2005) 134419.
[11] D. Heslop, A.R. Muxworthy, J. Magn. Magn. Mater. 288 (2005) 155.
[12] I.D. Mayergoyz, Mathematical Models of Hysteresis, Springer, New York, 1991.
[13] J.W. Diggle, et al., Chem. Rev. 69 (1969) 365.
[14] K. Nielsch, et al., Nano Lett. 2 (2002) 677.
[15] O. Jessensky, F. Müller, U. Gösele, J. Electrochem. Soc. 145 (1998) 3735.
[16] R.M. Metzger, et al., IEEE Trans. Magn. 36 (2000) 30.
[17] M. Vázquez, et al., Eur. Phys. J. B 40 (2004) 489.
[18] L. Ba, W.S. Li, J. Phys. D: Appl. Phys. 33 (2000) 2527.
[19] K. Nielsch, et al., J. Magn. Magn. Mater. 249 (2002) 234.
[20] D.R. Cornejo, E. Padrón-Hernández, J. Magn. Magn. Mater. 316 (2007) e48.
[21] H. Chiriac, et al., J. Magn. Magn. Mater. 316 (2007) 177.
[22] R. K Dumas, et al., Phys. Rev. B 75 (2007) 134405.